First measurements of the longitudinal bunch profile of a 28.5 GeV beam using coherent Smith-Purcell radiation

V. Blackmore, G. Doucas,* C. Perry, and B. Ottewell
The John Adams Institute, Department of Physics, Denys Wilkinson Building, University of Oxford, Oxford, United Kingdom

M. F. Kimmitt
Physics Centre, University of Essex, Colchester, United Kingdom

M. Woods, S. Molloy, and R. Arnold
SLAC, Stanford University, Stanford, California 94305, USA
(Received 6 December 2008; published 18 March 2009)

Coherent Smith-Purcell (SP) radiation originating from three different gratings has been measured at End Station A, SLAC, and has been used to reconstruct the time profile of the electron bunches. The beam energy during these experiments was 28.5 GeV ($\gamma \cong 55\,773$) and the number of electrons in the bunch was $0.9–1.4 \times 10^{10}$. The spectral distribution of the radiated energy was measured by means of an array of 11 pyroelectric detectors. Typical values of the FWHM of the bunch length are about 2.5 ps, but sharper peaks with FWHM less than 2.0 ps have also been observed. The longitudinal profile also varies with accelerator conditions and can best be approximated by a superposition of 3–4 Gaussian curves. Some typical profiles are presented, together with a discussion of the limitations and strengths of coherent SP radiation as a diagnostic tool. It is concluded that SP radiation offers excellent prospects in this respect, not only in the picosecond range, but potentially in the femtosecond range as well.

DOI: 10.1103/PhysRevSTAB.12.032803 PACS numbers: 41.60.−m, 41.85.Ew, 41.75.Ht

I. INTRODUCTION

The longitudinal (time) profile of two colliding bunches is a significant parameter that enters into the calculation of a number of beam-beam effects (e.g. beamstrahlung, beam deflection) at the collision point and, hence, it plays a crucial role in the optimization of the collider luminosity [1,2]. It is also of great interest in the context of x-ray free electron lasers (FELs). In the case of the International Linear Collider, the bunch length is likely to be of the order of a picosecond, while x-ray FEL bunches are likely to be in the 100 fs range. Accelerators based on the extremely high field gradients created in a plasma, either by means of a laser or an electron beam, are currently attracting a lot of interest. In this case, the bunch length of the high energy electron beam is likely to be of the order of a few femtoseconds. In all cases, there is a need for high quality, nondestructive diagnostics for the time profile of the bunch; ''single-shot'' capability may also be an advantage, in certain cases.

The three methods of approaching this problem can be broadly classified as: (a) electro-optic sampling of the bunch; (b) deflection and rotation of the bunch so that its longitudinal profile is transformed to a transverse dimension; (c) use of a coherent radiative process, such as transition, diffraction, or synchrotron radiation, so that a measurement of the spectral distribution of the radiated energy can be used to reconstruct the time profile of the bunch. The present paper deals with experiments carried out using another, related, radiative process, Smith-Purcell (SP) radiation [3]. This is the term used to describe the radiation emitted through the interaction of a charged particle beam (electrons, in our case) with a nearby periodic metallic structure, the grating. The details of this process can be found in numerous publications [4–20] and in the references contained therein, so we restrict ourselves to a brief summary of its essential features.

A. General comments on coherent Smith-Purcell radiation

A schematic of the SP process is shown in Fig. 1, which also shows the axis convention used in this paper. A single electron (or an electron bunch) is traveling past a grating of period l with velocity βc and at a height x_0 above the grating surface. As a result of the coupling between electron and grating, radiation is emitted from the grating surface. The first important relationship in SP radiation connects the wavelength λ of the radiation with the period l of the grating:

$$\lambda = \frac{l}{n}\left(\frac{1}{\beta} - \cos\theta\right), \tag{1}$$

where θ is the observation angle relative to the beam direction, β is the relativistic velocity of the particle, and n is the order of the emitted radiation. The grating, therefore, acts as its own monochromator and disperses the radiation according to the observation angle; short wavelengths appear in the forward direction, long ones in the

*Corresponding author.

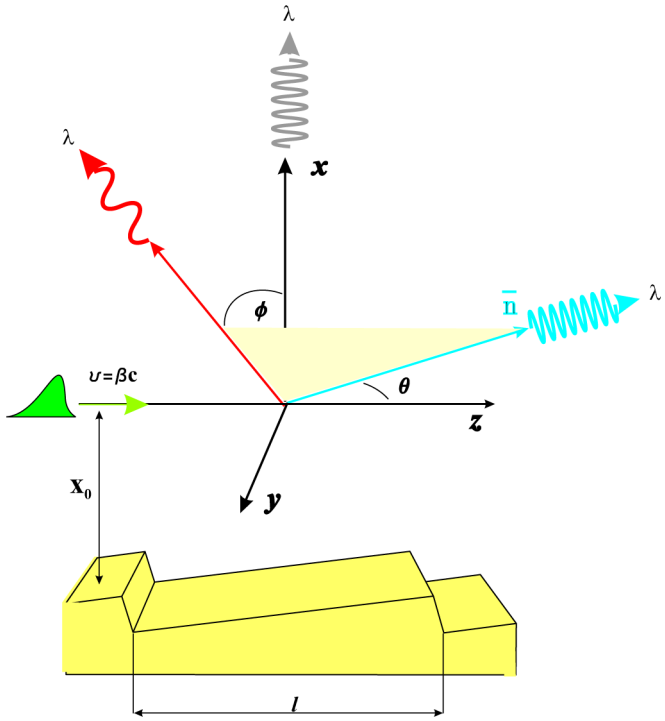

FIG. 1. (Color) Schematic of the Smith-Purcell radiative process and definition of the coordinate system.

backward, and at $\theta = 90°$ the emitted wavelength (for order 1) is equal to the period of the grating. It is assumed that the observation is taking place in the x-z plane ($\phi = 0$) and that the observer is sufficiently far away from the grating.

In the case of a narrow bunch consisting of N_e electrons, the emitted energy per solid angle is given by the well-known expression

$$\left(\frac{dI}{d\Omega}\right)_{N_e} = \left(\frac{dI}{d\Omega}\right)_1 (N_e S_{\text{inc}} + N_e^2 S_{\text{coh}}), \tag{2}$$

where $(dI/d\Omega)_1$ is the energy emitted by a single electron. The terms inside the second parenthesis on the right-hand side of Eq. (2) describe the way in which the contributions of individual electrons add up to the total intensity. In the case of a tightly bunched beam, the first term in the parenthesis becomes negligible compared to the second and the yield is proportional to the square of the number of electrons. This is the "coherent" regime and the transition to full coherence starts, approximately, when the bunch length is equal to the wavelength of the emitted radiation. These comments apply, of course, to all radiative processes but the interesting feature of SP radiation is the fact that by a suitable choice of the grating period the emission can be made coherent. Assuming that the charge distribution $q(x, y, t)$ inside the bunch can be expressed by three uncorrelated distributions

$$q(x, y, t) = X(x)Y(y)T(t),$$

the coherent integral is given by

$$S_{\text{coh}} = \left| \int_0^\infty X e^{-(x-x_0)/\lambda_e} dx \right|^2 \left| \int_{-\infty}^\infty Y e^{-ik_y y} dy \right|^2 \times \left| \int_{-\infty}^\infty T e^{-i\omega t} dt \right|^2. \tag{3}$$

In the above expression, ω is the frequency of the radiation and $k_y = k \sin\theta \sin\phi$ is the y component of the wave vector (k). The quantity λ_e is discussed in the following paragraph. Therefore, a measurement of the spectral distribution of the radiated energy in the coherent regime allows the calculation of the Fourier transform of the time profile of the bunch through the relationship

$$\left(\frac{dI}{d\Omega}\right)_{N_e} \cong \left(\frac{dI}{d\Omega}\right)_1 N_e^2 S_{\text{coh}} \approx \left(\frac{dI}{d\Omega}\right)_1 N_e^2 \left| \int_{-\infty}^\infty T e^{-i\omega t} dt \right|^2$$

and setting $\left| \int_{-\infty}^\infty T e^{-i\omega t} dt \right|^2 \equiv \rho^2(\nu)$, where $\nu = 2\pi/\omega$

$$\left(\frac{dI}{d\Omega}\right)_{N_e} \cong \left(\frac{dI}{d\Omega}\right)_1 N_e^2 \rho^2(\nu). \tag{4}$$

The problem then comes down to the calculation of the one-electron spectral yield $(dI/d\Omega)_1$. The various theoretical approaches to the solution of this problem that have been suggested over the years can be divided into two broad categories: (a) the emission process is described in terms of waves reflected by the grating surface from the evanescent waves that accompany the electron beam [7,21–23] or (b) the emission is due to the acceleration of surface charges induced on the grating surface by the electrons in the bunch [3,10,24–26]. A detailed description of the various theories is beyond the scope of this paper, but in all cases there is an exponential dependence of the yield on the bunch-grating spacing; this exponential factor also involves a parameter that describes the coupling efficiency between beam and grating. This is referred to as the "coupling factor" or "evanescent wavelength" and is usually defined as

$$\lambda_e = \frac{\beta\gamma\lambda}{2\pi\sqrt{1 + \beta^2\gamma^2 \sin^2\theta \sin^2\phi}}.$$

We note, incidentally, that although it is sometimes assumed that very high values of γ imply a high value for λ_e, this is only true for observations in the $\phi = 0$ plane; otherwise

$$\lambda_e \cong \frac{\lambda}{\sin\theta \sin\phi}.$$

Since all detectors have a finite acceptance in the azimuthal direction, λ_e will effectively depend on the wavelength for all practical applications.

It is important to note that the fundamental difference between theories lies in their predictions for the radiated intensity at very high beam energies. At low energies the theories appear to be in broad agreement. Recent experi-

ments, for example, with a 15 MeV beam [27] have demonstrated good agreement between measured power and the predictions of the extended field integral equation (EFIE) theory [19,23]; the same comment can be made about experiments at 1.8 MeV that were analyzed with the surface current theory [28]. The specific difference between theories in the highly relativistic regime lies in the expected behavior of the dimensionless "grating efficiency," or "radiation factor" R^2. In the surface current model this factor is rather insensitive to γ [26], increasing slightly with energy up to about 50 MeV and being essentially constant thereafter: the yield is expected to increase with energy. The predictions of the diffracted wave theories, on the other hand, are exactly the opposite: the radiation factor R^2 (and the radiated intensity) are expected to decrease rapidly with beam energy [22].

The present paper is based on the surface current model for SP radiation. We believe that this theory is physically transparent, computationally easier, and more importantly, is consistent with the well-established behavior of related radiative processes such as transition radiation. In this theory, the one-electron spectral yield is given by [24]

$$\left(\frac{dI}{d\Omega}\right)_1 = 2\pi e^2 \frac{Z}{l^2} \frac{n^2\beta^3}{(1-\beta\cos\theta)^3} \exp\left[-\frac{2x_0}{\lambda_e}\right] R^2. \quad (5)$$

The quantity Z in this expression is the grating length, n is the order of the emitted radiation, and the other quantities have been already defined. R^2 is a complicated function of the grating profile, the emission angle, and the order of the radiation and is calculated numerically.

In a previous paper [29], we presented the first observations of SP radiation at 28.5 GeV. We now present a more detailed analysis of the data and the exploitation of the spectral distribution of SP radiation in order to determine the longitudinal profile of the electron bunch at SLAC. The rest of the paper is structured as follows: Sec. II deals with the experimental arrangement; Sec. III with the extraction of the SP signal from the raw data; Sec. IV with the determination of the time profile of the bunch; and Sec. V presents the summary and the conclusions of this work.

II. EXPERIMENTAL

The experiments described in this paper were carried out at End Station A (ESA) of the Stanford Linear Accelerator Center (SLAC). The beam energy was 28.5 GeV ($\gamma \cong 55773$) and the bunch structure consisted of a single bunch, with a repetition rate of 10 Hz. The number of electrons per bunch, measured about 20 m upstream from the SP apparatus, varied between $0.9–1.4 \times 10^{10}$. The transverse size of the bunch was measured with two wire scanners located about 10 m on either side of the SP apparatus and was found to have $\sigma_x = 0.49$ mm and $\sigma_y = 0.14$ mm. The normalized beam emittance is 310 mm mrad in the horizontal direction and 13 mm mrad in the vertical [30].

The experimental apparatus consisted of: (a) a vacuum chamber which contained the gratings and (b) a detection system for the far infrared (FIR) radiation, located outside the chamber. The main elements of the FIR detection system were the filters, the light concentrators (Winston cones), the pyroelectric detectors, and the data acquisition system (DAQ). The details of the apparatus are discussed in the following sections.

A. The vacuum chamber

The chamber was a cylinder with an internal diameter of about 100 mm and a total insertion length in the beam line of about 0.5 m. It contained a remotely operated "carousel" which could accommodate four gratings. The first three positions were occupied by gratings with periodicities of 0.5, 1.0, and 1.5 mm. The period of each grating consisted of two facets. The blaze angle of the first facet was 40°, 35°, and 30°, respectively; the second facet was perpendicular to the first. Although the choice of blaze angle does affect the efficiency of the grating, the angles were chosen for ease of manufacture, rather than maximum output. The gratings were made of aluminum and were 40 mm long and 20 mm wide. The fourth position was occupied by a "blank". This was a smooth piece of aluminum, i.e. without any periodicity, and whose overall dimensions were identical to those of the gratings. The purpose of this blank is explained in Sec. III. Figure 2(a) shows the vacuum chamber and Fig. 2(b) the gratings inside the chamber. The orientation of the apparatus is such that the vertical to the grating surface coincides with the horizontal (x) direction. Therefore, the plane of the grating surface is the y-z plane. The control mechanism allowed the selected grating (or the blank) to move horizontally and be brought to the desired position, close to the beam centroid. Most of the work reported here was carried out with the grating positioned about 3 mm away from the beam. The SP radiation emerged to the outside world through a z-cut crystalline quartz window with dimensions of 210 mm × 50 mm × 6 mm.

B. Filters

The filters used in this experiment are of the waveguide array plate (WAP) type [31–33]. Each filter consisted of a brass disk with a diameter of 21 mm. The disk had a number of holes drilled through it. The diameter and spacing of these holes, as well as the thickness of the disk determine the transmission properties of the filter. The main characteristic of this type of filter, which makes them highly suitable for this application, is that they have very high transmission efficiencies at the design wavelength and a very sharp cutoff on the long wavelength side. The drop in efficiency on the short wavelength side is not as sharp. It is evident that a number of these filters are required in order to match the expected wavelengths from the three different gratings. Therefore, it is necessary to

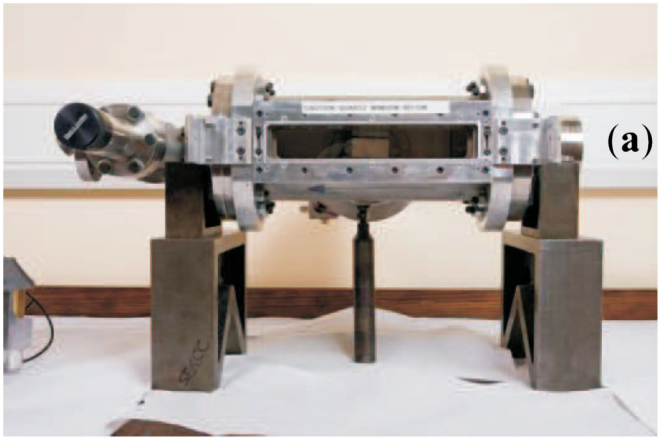

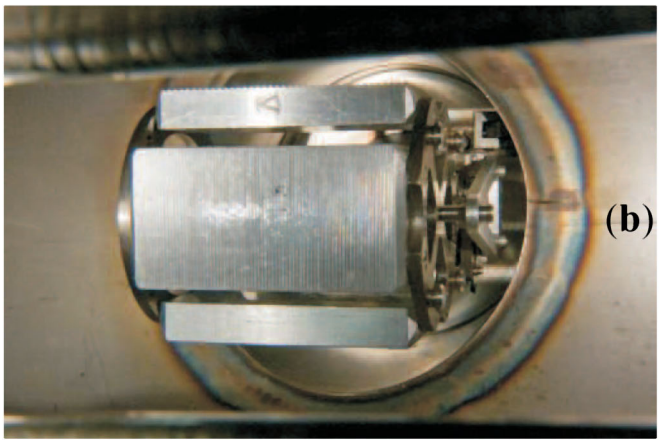

FIG. 2. (Color) (a) The vacuum chamber with the crystalline quartz window and (b) one of the gratings, inside the chamber.

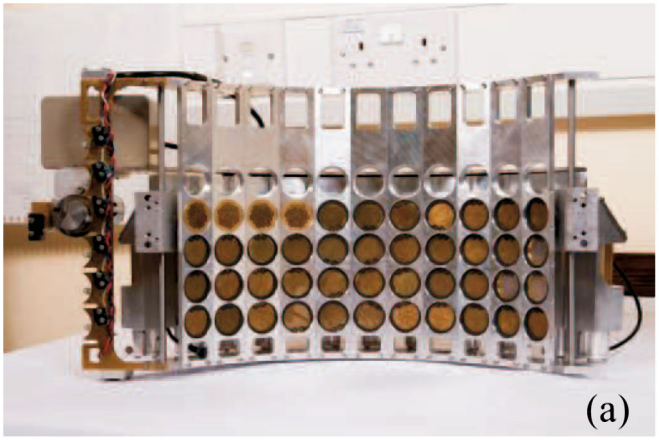

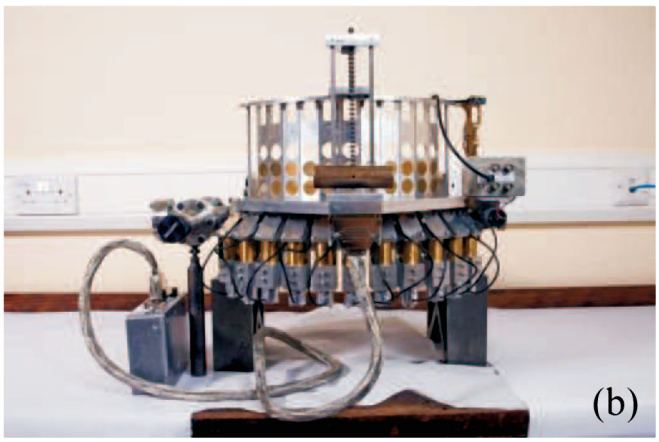

FIG. 3. (Color) (a) The filter changing mechanism and (b) the complete experimental apparatus. The box on the left is the DAQ system.

change the set of filters every time a different grating is inserted into the beam path. A previous experimental run at SLAC had demonstrated clearly that this should be done as speedily as possible in order to avoid any significant drift in beam conditions. In order to achieve this, a remotely controlled system was designed that allowed for the appropriate set of filters to be brought into use in a matter of a few tens of seconds. The system consisted of a metal screen with six rows of filters [see Fig. 3(a)]. Starting from the bottom, the rows correspond to filters for: (i) the 1.0 mm grating; (ii) the 0.5 mm grating, which are also good for orders 2 and 3 from the 1.0 mm and 1.5 mm gratings, respectively; (iii) order 2 from the 1.5 mm grating; (iv) the 1.5 mm grating.

Row five has no filters at all while "row 6" (top of the screen) is actually solid aluminum which, when inserted into the light path, provides a measurement of the irreducible background of the measuring system. This filter changing mechanism fulfilled its design criteria and proved to be a very useful modification to the experimental arrangement. Figure 3(b) shows the complete experimental arrangement, with the filter changer mounted onto the chamber. A typical (power) transmission curve for one of the WAP filters is shown in Fig. 4.

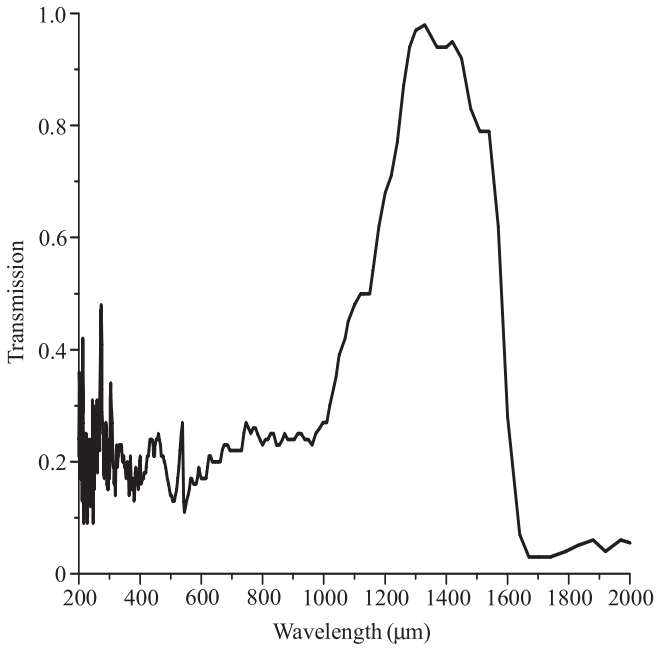

FIG. 4. Measured transmission curve of the filter used on the 90° port, with the 1.5 mm grating.

C. Light concentrators (Winston cones)

Light concentrators, in the form of Winston cones, have already been described in the literature, for a number of different applications [34,35]. We have designed and fabricated our own concentrators, whose characteristics are matched to those of the expected SP radiation. The cones were fabricated out of brass and have an entry diameter of 21 mm and an exit diameter of 2.8 mm. The length of each cone is 71.5 mm and the internal profile is that generated by the rotation of a parabola around an axis that is inclined at a certain angle relative to the axis of symmetry of the parabola. The cone is capable of transmitting rays entering with an angle of up to 6.3° in which case the maximum exit angle is 60°. The latter angle is determined by the properties of the pyroelectric detector. The sizes of the entry and exit apertures define the maximum theoretical concentration factor for the cone; this is equal to 56 in this case. It should be noted that, because of its limited angular acceptance and the rather small size of its exit aperture, the cone itself is quite an efficient filter against long wavelength ($\geq$ 3 mm) radiation.

D. Pyroelectric detectors

The emitted SP radiation was detected by an 11-detector array of room temperature, pyroelectric detectors [36]. Although less sensitive than cryogenic detectors, they are very compact and inexpensive. They are sensitive to radiation from below 0.1 μm to well into the mm range. Each detector has an active area of 2 mm in diameter and was placed as close as possible ($\sim$ 0.5 mm) to the exit of the corresponding cone. The 11 cone-detector assemblies were mounted on a supporting bridge and arranged so as to observe radiation at angles in the range 40°–140° relative to the beam direction. In order to avoid a direct line of sight between the cone entry and any x rays originating inside the chamber, the cone entry was rotated by 90° relative to the incoming light and a 45° mirror was used to reflect the light into the cone entry aperture (Fig. 5). The main benefit of this arrangement was that it allowed the detectors to be screened behind lead blocks. The distance between the grating surface and the cone entry was about 230 mm. Therefore, the detector cannot be considered as being at infinity and the light entering the cone is not strictly monochromatic. In fact, the angular acceptance in the θ direction is $\pm$6.3° and in the ϕ (azimuthal) direction $\pm$5.0°. The solid angle subtended by the cone entrance is approximately 6.5 msr.

Detailed measurements of the spectral response of our detectors were carried out at the Rutherford Appleton Laboratory (RAL). These are again beyond the scope of this paper, but their conclusions are discussed in Sec. III.

E. The data acquisition system (DAQ)

The electronics used in this experiment have already been described in the literature [29] and, therefore, we restrict ourselves to a brief summary. There were a total of 14 channels, eleven for the active detectors, two for the reference detectors, and one for a PIN diode used to monitor the x rays. Each channel had a charge sensitive preamp with a junction field-effect transistor (JFET) input, which drove its own 14 bit analog-to-digital converter sampling at 400 kSa/s. Because of the sensitivity of the JFETs to x rays, it was decided to separate them from the detectors so that they could be properly shielded with lead bricks. The electronics were housed in a small aluminum box [see Fig. 3(b)], which also included signal digitization with control and readout over a slow serial link. Control and readout of the grating change and position was also included in the same box. The filter changing mechanism was a late addition and was run from a separate remote manual control box. A bundle of small coaxial cables, about 1.5 m long and placed inside a braided copper shield, connected the detectors to the DAQ box. Although this introduced an additional capacitance and degraded the noise performance, it was deemed to be acceptable. An RS232 link to a remote laptop computer controlled the unit and read out the data. The only software required was a standard terminal emulator program. The returned data were logged to a file for subsequent analysis, while the on-screen display gave an adequate presentation of the data being taken.

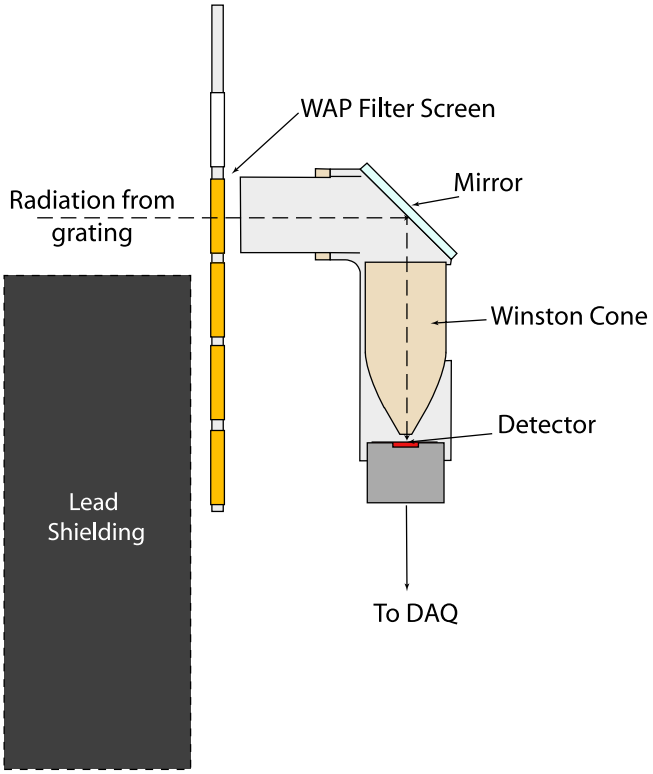

FIG. 5. (Color) Schematic of the detector-Winston cone arrangement.

III. EXTRACTION OF THE SMITH-PURCELL SIGNAL

Various wavelengths, arising from different processes, can be reflected inside the chamber and can find their way into the detection system; some of these wavelengths may coincide with the expected SP wavelengths. The most probable source for this ''background'' is diffraction radiation from the various upstream apertures. In addition, the insertion of the carousel structure itself generates diffraction radiation. Therefore, it is essential to account for this potential contribution to the true SP signal. This was achieved through the use of the previously mentioned ''blank.'' Insertion of the blank, instead of a grating, provides a measurement of all the background contributions to the expected SP signal, which are not related to the existence of a periodic structure. Hence, the difference ''grating minus blank'' is taken to be the true SP signal.

These considerations dictated the following procedure for collecting data. A grating was inserted close to the beam and the corresponding set of filters was moved in front of the cone entry. The data acquisition system collected data for about 1 min, during which time about 600 bunches had gone past the grating. Without changing the filter set, the blank was then moved into position and data were collected for a further 1 min. The whole process was then repeated for the other two gratings. The SP signal is the difference between the averages obtained from the grating and from the blank.

A. Transmission factors

The signals reaching the detectors have to be corrected for losses incurred while covering the distance between the grating and the detectors. These corrections, or transmission factors, were arrived at either by calculation or by direct calibration measurements carried out at RAL. As indicated earlier, a full account of this work is outside the scope of this paper and we only present a summary of the main points.

1. Crystalline quartz window.—This material has a refractive index $n = 2.1$. The multiple reflection losses are wavelength dependent and can be calculated using formulas from the literature [37]. We have assumed that both polarizations are possible and have taken the average of the estimated power transmission factor. We have also assumed that there is an approximate loss of about 25% inside the quartz. It should be noted that quartz is opaque in the mid-infrared and starts transmitting again above $\sim 50\ \mu$m.

2. Wire grid and black polyethylene.—A copper wire grid (2 mm mesh size) was placed against the quartz window, on the air side, with the intention of providing screening against any long wavelength radiation escaping from the chamber; in actual fact, its existence turned out to be an unnecessary complication. It was not possible to carry out a sufficiently detailed measurement of its transmission properties in the wavelength region of interest (approximately 0.5–2.6 mm). Measurements carried out using terahertz time domain spectroscopy (THz-TDS) could only cover the wavelength range up to ~ 1.8 mm and gave a transmission factor of about 0.5; this value has been used throughout the analysis but it could be underestimating the losses at $\lambda > 1.8$ mm. A layer of black polyethylene was also placed against the quartz window to act as a shield against visible light; its transmission is estimated at about 90%.

3. Filters.—The characteristics of all the filters used in this experiment were determined either by THz-TDS or through the use of a Fourier transform spectrometer and a liquid helium cooled InSb detector. Typical transmission values at the design wavelength are in the 70%–80% region.

4. Winston cones.—The theoretical concentration factor of the cone (56 in this case) cannot be achieved in practice, even for an ideal concentrator. The efficiency of the cone-detector assembly is bound to be smaller than that, primarily because of the nonzero spacing between cone exit and detector surface and the fact that the detector diameter (2 mm) is smaller than the cone exit diameter (2.8 mm). The cone-detector efficiency also depends on the wavelength of the radiation. This is particularly important in the long wavelength region since the maximum expected SP signal has a wavelength of about 2.6 mm, which is close to the size of the exit aperture. Therefore, a further reduction in efficiency is to be expected. A series of measurements were undertaken at the Space Science and Technology Department of the Rutherford Appleton Laboratory (RAL) in order to determine the properties of the cone. In summary, these measurements indicate that the efficiency of the cone-detector system up to about 2.2 mm is equal to 0.465; thereafter, it declines with wavelength down to about 0.21 at 2.6 mm. Therefore, at 2.6 mm, only 21% of the flux entering the cone aperture will be detected by the pyroelectric detector.

5. Pyroelectric detectors.—The determination of the time profile of the bunch relies on the measurement of the wavelength distribution of the radiated energy. In a system where multiple detectors are used, like the one described here, it follows that it is essential to have not only an absolute measurement of the responsivity of the detectors used but, also, a measurement of the relative responsivity of the detectors, *at the wavelengths that each detector is expected to receive*. This is a complicated task, especially in the far infrared, where absolute measurements are notoriously difficult and the availability of suitable sources is very limited. It should also be noted that, although pyroelectric detectors are supposed to have a flat spectral response, there have been reports in the literature that this may not be true [38]. The ideal solution to this problem would be a calibration of each detector against a Golay cell, taken over as many discreet wavelengths as

possible, in the wavelength region of interest (0.5–2.6 mm); this statement assumes, of course, that the Golay cell itself has a flat spectral response. We have been able to carry out this cross referencing of the detectors in the region 1.0–2.6 mm using two different photomixer diodes. In the region 0.5–1.0 mm we were only able to obtain an average value, using a blackbody as a source. We arbitrarily defined 1.5 mm as the reference wavelength and the detector located at $\theta = 90°$ as the reference detector. All detector responsivities, at the wavelength that they are expected to observe, were referred to that of the 90° detector, at 1.5 mm. An absolute calibration of the reference detector was also obtained.

6. Other losses.—A transmission efficiency of 80% has been calculated for the 45° mirror that is used to deflect the radiation by 90°, into the cone entrance. Any possible losses due to absorption in the atmosphere have been neglected, because of the short path length (~ 300 mm).

In summary, only a small fraction of the light radiated from the grating is actually detected. The exact value of the overall transmission efficiency between grating and detector depends on the wavelength of the radiation; typically, for radiation of $\lambda = 1.5$ mm it is about 8%.

B. Uncertainty estimates

The dominant sources of uncertainty in these measurements are the systematic ones. We estimate that the relative calibration of the detector carries an uncertainty of about $\pm 30\%$ and a similar uncertainty must be associated with the estimate of the losses through the wire grid over the quartz window. This is particularly true for the longer wavelengths. Assuming that the other estimates have a combined uncertainty of about $\pm 20\%$, we deduce a value of about $\pm 50\%$ for the total uncertainty in the experiments reported here. It would be difficult to improve on the calibration uncertainties in the far infrared part of the spectrum but it is possible to improve on those arising from the quartz-grid assembly. Thus, for a possible future experiment, it would be realistic to expect a total uncertainty in the region of $\pm 35\%$.

The statistical uncertainties are usually small compared to the systematic ones, apart from the "shallow" observation angles (especially in the forward direction), where they can become comparable to the systematic uncertainties. This is particularly true for the short period grating, when the signal level is low and the signal-to-noise ratio is rather poor.

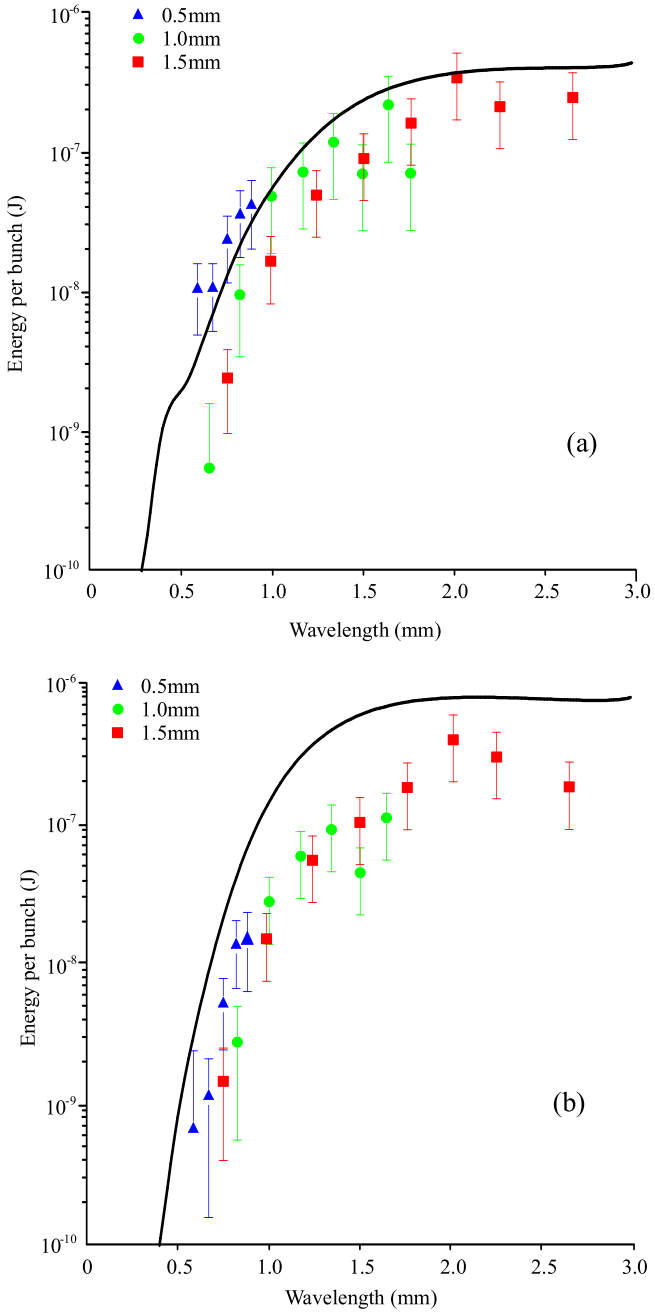

FIG. 6. (Color) Spectral distribution of coherent SP radiation measured with three gratings on: (a) the 13/07/07, between 0641–0741 and (b) the 18/07/07, between 0404–0517. The number of electrons per bunch was $\cong 0.9 \times 10^{10}$ and $\cong 1.1 \times 10^{10}$, respectively. See text (Sec. IV C) for details of the solid lines.

IV. DETERMINATION OF THE BUNCH TIME PROFILE

A. General comments

A number of measurements were made over the period 13–20/07/07. Figure 6(a) shows the spectral distribution of coherent SP radiation derived from a cycle of measurements taken between 06:51 and 07:14 on 13/07/07 using all three gratings; the number of electrons (N_e) in the bunch during that period was $\cong 0.9 \times 10^{10}$. A second set of measurements, taken between 04:40–05:17 on 18/07/07 and with $N_e \cong 1.1 \times 10^{10}$, is shown in Fig. 6(b). The error bars are the combined systematic and statistical uncertainties. Having derived the spectral distribution of the coher-

ent SP radiation, one can then proceed to the determination of the longitudinal (time) profile of the bunch that gave rise to this radiation. Since the measurements determine the *square* of the Fourier transform of the time profile, there is no direct information about the phase and, hence, it is not possible to carry out the inverse Fourier transform in order to recover the time profile $T(t)$. Therefore, there are two options.

The first approach is to assume a number of plausible profiles, derive their spectral distribution, and then compare them to the measured values [28,39]. This is a valid procedure but there is a finite number of such, rather simple, ''templates'' that can be created and there is always the possibility that there may exist another profile that gives an even better fit to the data.

The alternative approach, which is the one followed in this paper, is to apply the Kramers-Kronig (KK), or dispersion, relations [40], which are applicable to a causal, linear system. The question, therefore, is whether a bunch of electrons does constitute such a system and, if so, how to apply the KK relations, given that only the magnitude of the Fourier transform is available from the measurements. Lai and Sievers were the first to suggest that a bunch of finite duration does obey causality (the ''output'' follows the ''stimulus'') and is also a linear system in the sense that the *field* of the bunch is N_e times the field of a single electron [41]. The missing phase could then be recovered by a technique suggested by Wooten [42] in connection with the problem of the complex reflectivity of solids. In the case of the bunch, however, there is an additional complication that renders the unambiguous determination of the phase impossible. This stems from the fact that the existence of zeros in the form factor cannot be excluded *a priori*. The phase that can be determined is the *minimal* phase $\psi(\nu_0)$ that is compatible with the data. A comprehensive description of the application of the KK analysis to the bunch profile problem can be found in Refs. [43–46]. We restrict ourselves to some general comments.

It is assumed that the bunch profile $T(t)$ is of finite duration and starts at time $t = 0$. Working in the complex frequency plane, it is possible to calculate $\psi(\nu_0)$ at the (real) frequency ν_0 from the expression

$$\psi(\nu_0) = \frac{2\nu_0}{\pi} \int_0^\infty \frac{\ln(\frac{\rho(\nu)}{\rho(\nu_0)})}{\nu_0^2 - \nu^2} d\nu, \tag{6}$$

where $\rho(\nu_0)$ is the measured form factor. However, this minimal phase will be equal to the true phase only if there are no (complex) frequencies at which the form factor becomes zero. If the form factor does have zeros, these will give rise to an additional contribution to the phase, the so-called Blaschke phase, which cannot be determined experimentally. Smooth functions with continuous derivatives will not have zeros and it has been suggested [44] that, for realistic bunch shapes, the minimal phase is an adequate approximation. In general, however, the possibility of zeros cannot be excluded and, hence, the KK analysis of the bunch profile cannot guarantee a unique determination of the bunch profile. Nevertheless, and in view of the comments made in Sec. III B, it is felt that the potential error in the calculation of the phase is likely to be less significant than the experimental uncertainties.

It is important to note that the above expression implies knowledge of the form factor over all frequencies. In the frequency range covered by the measurements, the form factor can be derived from the data points through the use of Eq. (4) where all the quantities, apart from the square of the form factor $\rho^2(\nu)$, are either measured or can be calculated. As stated earlier, this assumes that the charge distributions in x, y, and z are uncorrelated and, moreover, that they are Gaussian in the x and y directions. The latter assumption is supported by the evidence of the wire scanner profiles of the bunch. However, since measurements are taken over a limited range of frequencies, it is necessary to interpolate between the data points and extrapolate beyond. This is an important issue, especially the extrapolation to low frequencies, which are crucial for the accurate reconstruction of the time profile. We have extrapolated to low frequencies using an expression of the form $\rho \cong \exp[-a(\nu - \nu_{\min})^2]\exp[b(\nu - \nu_{\min})]$, where $\nu_{\min}$ is the minimum measured frequency and the coefficients a and b have been determined so as to ensure that $\rho \rightarrow 1$ when $\nu \rightarrow 0$ and that the extrapolating function matches the data value (and the slope) at $\nu_{\min}$. The high frequency extrapolation is a simple fourth power decay.

We note here a clear advantage offered by SP radiation, compared to other radiative processes. This is the use of multiple gratings in order to increase the frequency range covered by the measurements, to match it to the expected bunch length and to aid the low frequency extrapolation. Although the present experiment used only three gratings, the possibility of more gratings, covering a broader spectral range, is available.

Having determined the minimal phase from (6), it is then possible to derive the time profile of the bunch by the expression:

$$T(t) = 2\int_0^\infty \rho(\nu)\cos[2\pi\nu t + \psi(\nu)]d\nu. \tag{7}$$

B. Expected accuracy of the KK reconstruction

The accuracy of the KK reconstruction has been tested by assuming an asymmetric profile, arising from the superposition of two Gaussians, and then calculating the expected spectral distribution from the three gratings used in this experiment. The calculated form factor ρ is then used to recover the original profile. The results of these simulations are summarized in Fig. 7.

Figure 7(a) is the reconstruction of a bunch with an assumed length of 3.3 ps (1.0 mm). The definition of ''bunch length'' used in this paper is the length of time

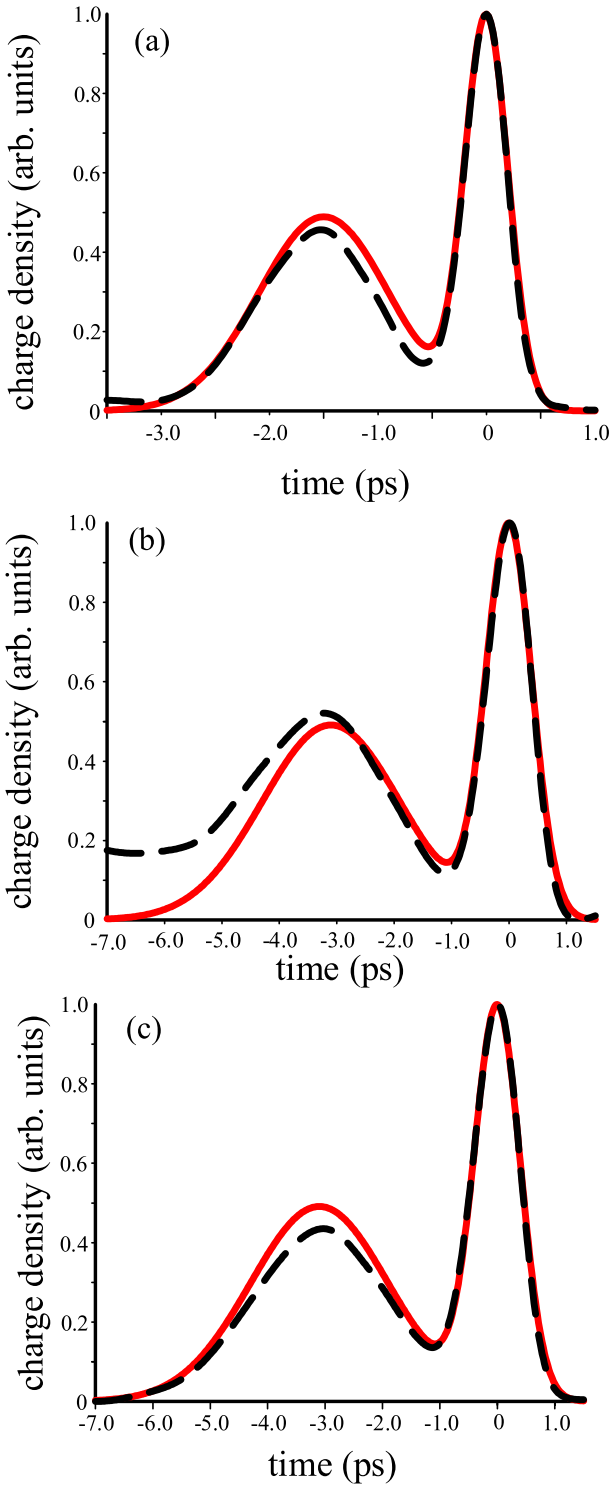

FIG. 7. (Color) Demonstration of the accuracy of the KK reconstruction of an asymmetric bunch profile, using the expected output from three different gratings. In all cases the original bunch consists of a superposition of two Gaussians. (a) bunch length = 3.3 ps, grating periods = 0.5, 1.0, and 1.5 mm; (b) bunch length = 6.6 ps, grating periods = 0.5, 1.0, and 1.5 mm; (c) bunch length = 6.6 ps, grating periods = 0.5, 2.0, and 14.0 mm. Solid line = original profile, dashed line = reconstructed profile.

between the two points in the distribution where the height is 5% of its peak value. The grating period (l) can be compared to the bunch length Δt through the use of a dimensionless parameter $\Gamma = l/\Delta t$. In this case we are using gratings with $\Gamma = 0.5$, 1, and 1.5 and the fit to the original profile is quite acceptable.

An even better fit could have been achieved through the use of more gratings and/or with grating periods that would cover a wider range of frequencies. In the present experimental setup, covering the angular range 40°–140°, a better spread of periods would have been in the approximate ratio 0.25:1:7. In Fig. 7(b) the assumed bunch length is 6.6 ps and the corresponding Γ values are 0.25, 0.5, and 0.75 which are not well matched to the bunch length, with a resultant poorer fit; the reconstructed profile does not drop to zero, probably because of the absence of the long wavelength data. However, it is worth noting that, although some of the details of the bunch structure are distorted, the overall bunch length is about right. A better spread of grating periods would have provided a much better fit [Fig. 7(c)].

C. Comments on the bunch profile at SLAC

The above procedure has been applied to the data shown in Figs. 6(a) and 6(b) and the results of the reconstruction are shown in Figs. 8(a) and 8(b), respectively. In the first case the FWHM of the main peak is 2.6 ps and the bunch length (as defined in this paper) is about 5.4 ps. The corresponding figures for the bunch of Fig. 8(b) are slightly shorter, 2.4 ps and 5.2 ps, respectively. These are fairly typical values, for the conditions prevailing at the time. Slightly longer lengths and more complicated profiles were also observed. The profiles in Figs. 8(a) and 8(b) can be approximated very well with a superposition of three Gaussians. We have not observed a profile approaching that of a simple Gaussian shape, although profiles consisting of a dominant peak followed by a trailing structure were observed (see Fig. 9). The FWHM in this case is 1.8 ps.

It is also of interest to check the consistency of the recovered profile with the predictions of the "surface current" model. This can be done in the following fashion. The three Gaussians that describe the profile of, say, Fig. 8(a) can be fed back into the analysis code in order to derive the expected spectral distribution of coherent SP radiation from such a bunch. This can then be compared with the measured data points. There are, of course, a number of possible errors and/or inaccuracies in this comparison, the most important being any inaccuracy in the KK reconstruction and errors in the estimate of the number of electrons actually going over the grating. The latter point could be significant in view of the fact that the bunch charge could only be measured 20 m *before* the grating and, hence, there is no way of knowing the exact number of electrons going over the grating. There is no doubt, how-

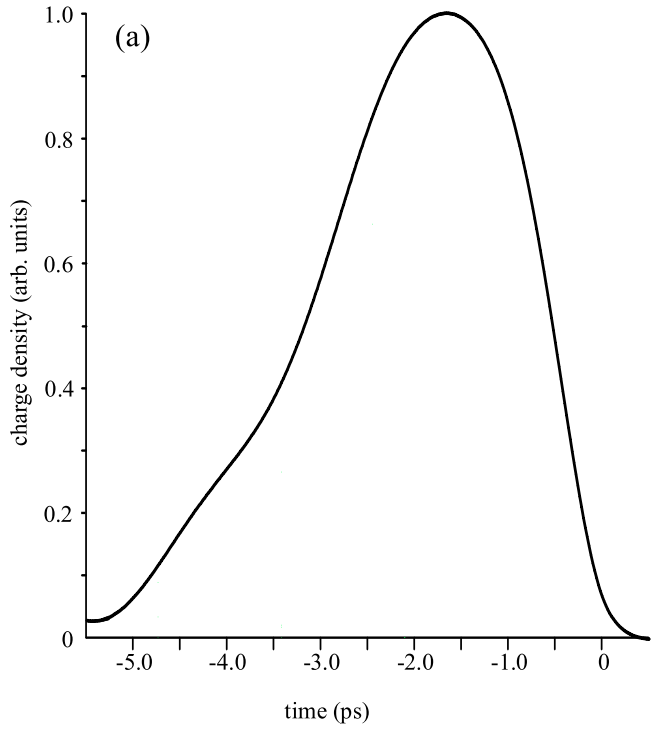

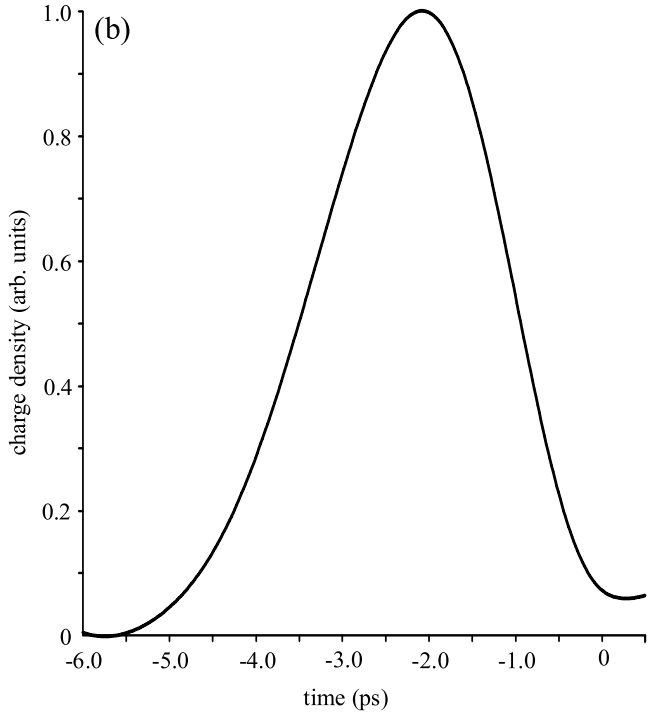

FIG. 8. (a) The reconstructed longitudinal profile corresponding to the data of: (a) Fig. 6(a) and (b) Fig. 6(b). The number of electrons per bunch was $\cong 0.9 \times 10^{10}$ and $\cong 1.1 \times 10^{10}$, respectively.

ever, that the grating was intercepting part of the beam halo. In addition, there could be errors in assuming uncorrelated charge distributions and errors in the calculation of the various losses. Therefore, we believe that agreement

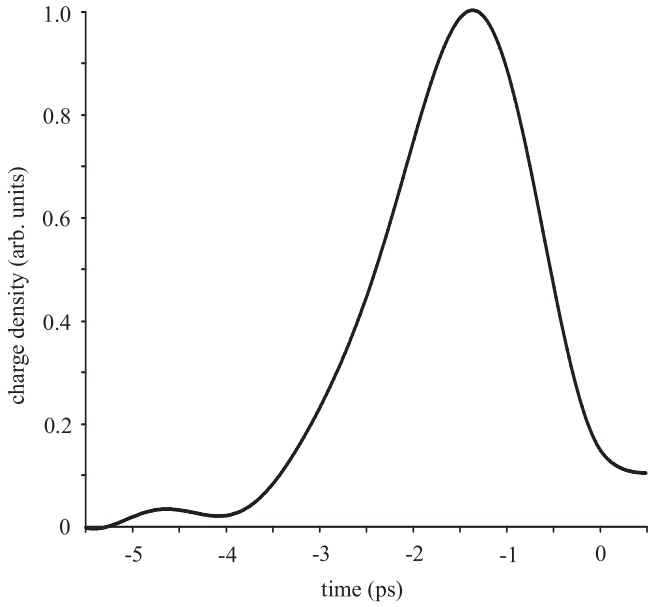

FIG. 9. Measured bunch profile with most of the charge concentrated in one peak. Data taken on 13/07/07, between 0451–0527. The number of electrons per bunch was $\cong 1.2 \times 10^{10}$.

within an order of magnitude should be considered, at this stage, as satisfactory. The solid line in Fig. 6(a) represents the expected (according to surface current theory) spectral distribution from the superposition of the three Gaussians. It can be seen that, in this case, agreement is quite good, whereas in the case of Fig. 6(b) there is a discrepancy by a factor of 3–4.

Disregarding for the moment the limitations imposed by the dimensions of the Winston cone, it is obvious from the preceding discussion on the accuracy of the KK determination of the minimal phase, that better results could have been obtained through the use of a longer period grating which would have extended the wavelength range covered by the measurements. Use of the higher emission orders ($n > 1$) would provide greater density of points within the measured wavelength range. Although there was provision in the experiment for the measurement of higher orders, the signal levels were usually rather low for the pyroelectric detectors.

V. SUMMARY AND CONCLUSIONS

We have carried out what we believe to be the first ever experiment on Smith-Purcell radiation in the multi-GeV regime and have used the coherent radiation in order to determine the time profile of the electron bunches at ESA, SLAC. Three different gratings and an array of 11 pyroelectric detectors were used for this purpose. The main conclusions of this work are as follows: (i) The radiated energy is in line with the predictions of the theory that describes SP radiation in terms of currents induced on the grating surface [Figs. 6(a) and 6(b)]. We consider this to be

a significant result in the sense that it lays to rest concerns that had been raised in the literature [18,22] about the validity of this theory in the extreme relativistic regime. Whether the surface current or the EFIE theory is more appropriate for the description of the emission process in the highly relativistic regime is a matter that merits further investigation [47]. (ii) The bunch profile has been reconstructed through the use of the KK technique for retrieval of the minimal phase of the Fourier transform. The bunch shape is not a simple Gaussian but can best be approximated by a superposition of 3–4 Gaussian curves. The FWHM of the dominant peak is, typically, around 2.4 ps but narrower peaks (FWHM < 2.0 ps), followed by a rather weak trailing part, have also been observed (Fig. 9). If we define as bunch length the time interval between the 5% points of the normalized charge distribution, then the measured bunch lengths varied between 5–6 ps. (iii) The measured bunch lengths are in line with those determined by the LOLA deflecting cavity [48]. However, since the two measurements were taken at different times and at different locations, it is not possible to say anything firmer than that. A direct comparison of SP with LOLA and with the electro-optic sampling technique would be highly desirable. (iv) The main challenge in these experiments was the calibration of the detectors in the far infrared and the detailed calculation of all the possible loss mechanisms between grating and detector(s). Further improvements in this area are possible, especially if suitable sources of FIR radiation in the sub-mm and mm region are available. (v) The use of multiple gratings is a major strength of the SP radiation. Only three gratings were used in the experiments reported here and the choice of their periodicities was not optimal. However, it is possible to design an experiment with more gratings and, hence, with even wider wavelength coverage.

We conclude that coherent SP radiation has some significant advantages as a bunch profile diagnostic tool: apart from the broad wavelength coverage that it can provide, it is also rather inexpensive to construct, has a small insertion length in the beam line, and is noninvasive; compared to diffraction radiation, it gives a stronger signal and it acts as its own monochromator. In addition, it also has a true ''single-shot'' capability for this type of measurement. There is a lengthy list of potential improvements to the experimental setup, but the ones we consider particularly important are the investigation of alternative detector arrays and the exploitation of the expected polarization of the SP radiation for the rejection of the background radiation. Therefore, the work presented here should be considered as a pilot experiment. Nevertheless, we believe that the capabilities of this technique have been demonstrated. Finally, we note that all indications are that the application of coherent SP radiation can be extended down to the few femtosecond range; this is the area of electron acceleration in a plasma wave, which is currently attracting considerable attention.

ACKNOWLEDGMENTS

The authors are grateful to Peter Huggard (Rutherford Appleton Laboratory) for his invaluable guidance and advice in all the detector calibration work. We are also grateful to Michael Johnston and his group at the Clarendon Laboratory for their assistance with the THz-TDS measurements. Thanks are due to Mike Tacon and the Oxford mechanical workshop for their skill and efficiency in the manufacture of quite complicated mechanical components of the system. We thank the SLAC experimental facilities and accelerator operations groups. This work is supported in part by U.S. Department of Energy Contract No. DEAC02-76SF00515. Finally, the financial support of STFC (formerly PPARC) under the LC-ABD Collaboration and of the John Adams Institute is gratefully acknowledged.

[1] R. Palmer, Report No. SLAC-PUB-4295, 1987.
[2] K. Yokoya and P. Chen, Beam-Beam Phenomena in Linear Colliders, U.S.-CERN Particle Accelerator School Lecture, 1990.
[3] S. J. Smith and E. M. Purcell, Phys. Rev. **92**, 1069 (1953).
[4] J. P. Bachheimer, Phys. Rev. B **6**, 2985 (1972).
[5] E. L. Burdette and G. Hughes, Phys. Rev. A **14**, 1766 (1976).
[6] P. M. van den Berg, J. Opt. Soc. Am. **63**, 689 (1973).
[7] P. M. van den Berg, J. Opt. Soc. Am. **63**, 1588 (1973).
[8] A. Gover, P. Dvorikis, and U. Elisha, J. Opt. Soc. Am. B **1**, 723 (1984).
[9] K. Mizuno, J. Pae, T. Nozokido, and K. Furuya, Nature (London) **328**, 45 (1987).
[10] J. C. McDaniel, D. B. Chang, J. E. Drummond, and W. W. Salisbury, Appl. Opt. **28**, 4924 (1989).
[11] I. Shih, W. W. Salisbury, D. L. Masters, and D. B. Chang, J. Opt. Soc. Am. B **7**, 345 (1990).
[12] G. Doucas, J. H. Mulvey, M. Omori, J. Walsh, and M. F. Kimmitt, Phys. Rev. Lett. **69**, 1761 (1992).
[13] J. Walsh, K. Woods, and S. Yeager, Nucl. Instrum. Methods Phys. Res., Sect. A **341**, 277 (1994).
[14] K. J. Woods, J. E. Walsh, R. E. Stoner, H. G. Kirk, and R. C. Fernow, Phys. Rev. Lett. **74**, 3808 (1995).
[15] J. H. Brownell, J. Walsh, H. G. Kirk, R. C. Fernow, and S. H. Robertson, Nucl. Instrum. Methods Phys. Res., Sect. A **393**, 323 (1997).
[16] J. Urata, M. Goldstein, M. F. Kimmitt, A. Naumov, C. Platt, and J. E. Walsh, Phys. Rev. Lett. **80**, 516 (1998).
[17] Y. Shibata, S. Hasebe, K. Ishi, S. Ono, M. Ikezawa, T. Nakazato, M. Oyamada, S. Urasawa, T. Takahashi, T. Matsuyama, K. Kobayashi, and Y. Fujita, Phys. Rev. E **57**, 1061 (1998).
[18] G. Kube, H. Backe, H. Euteneuer, A. Gendel, F. Hagenbuck, H. Hartmann, K. H. Kaiser, W. Lauth, H. Schöpe, G. Wagner, and Th. Walcher, Phys. Rev. E **65**, 056501 (2002).
[19] S. E. Korbly, A. S. Kesar , J. R. Sirigiri, and R. J. Temkin, Phys. Rev. Lett. **94**, 054803 (2005).

[20] H. L. Andrews, C. H. Boulware, C. A. Brau, and J. D. Jarvis, Phys. Rev. ST Accel. Beams **8**, 050703 (2005).
[21] G. Toraldo di Francia, Nuovo Cimento **16**, 61 (1960).
[22] O. Haeberlé, P. Rullhusen, J.-M. Salomé, and N. Maene, Phys. Rev. E **49**, 3340 (1994).
[23] A. S. Kesar, Phys. Rev. ST Accel. Beams **8**, 072801 (2005).
[24] J. H. Brownell, J. E. Walsh, and G. Doucas, Phys. Rev. E **57**, 1075 (1998).
[25] S. R. Trotz, J. H. Brownell, J. E. Walsh, and G. Doucas, Phys. Rev. E **61**, 7057 (2000).
[26] J. H. Brownell and G. Doucas, Phys. Rev. ST Accel. Beams **8**, 091301 (2005).
[27] A. S. Kesar, R. A. Marsh, and R. J. Temkin, Phys. Rev. ST Accel. Beams **9**, 022801 (2006).
[28] G. Doucas, M. F. Kimmitt, A. Doria, G. P. Gallerano, E. Giovenale, G. Messina, H. L. Andrews, and J. H. Brownell, Phys. Rev. ST Accel. Beams **5**, 072802 (2002).
[29] V. Blackmore, G. Doucas, C. Perry, and M. F. Kimmitt, Nucl. Instrum. Methods Phys. Res., Sect. B **266**, 3803 (2008).
[30] SLAC PUB 11988, http://www.slac.stanford.edu/pubs/slacpubs/11000/slac-pub-11988.html.
[31] R. Ulrich, Infrared Phys. **7**, 1987 (1967).
[32] C. Winnewisser, F. Lewen, and H. Helm, Appl. Phys. A **66**, 593 (1998).
[33] C. Winnewisser, F. T. Lewen, M. Schall, M. Walther, and H. Helm, IEEE Trans. Microwave Theory Tech. **48**, 744 (2000).
[34] A. Rabi and R. Winston, Appl. Opt. **15**, 2880 (1976).
[35] G. Doucas, S. Gil, N. A. Jelley, L. McGarry, M. E. Moorhead, N. W. Tanner, and C. E. Waltham, Nucl. Instrum. Methods Phys. Res., Sect. A **370**, 579 (1996).
[36] Eltec, model 400-0.
[37] O. S. Heavens, *Optical Properties of Thin Solid Films* (Butterworth Scientific Publications, London, 1955).
[38] W. Zhu, J. R. Izatt, and B. K. Deka, Appl. Opt. **28**, 3647 (1989).
[39] S. E. Korbly, A. S. Kesar, R. J. Temkin, and J. H. Brownell, Phys. Rev. ST Accel. Beams **9**, 022802 (2006).
[40] J. D. Jackson, *Classical Electrodynamics* (John Wiley & Sons, New York, 1975), 2nd ed., Chap. 7.
[41] R. Lai and A. J. Sievers, Phys. Rev. E **50**, R3342 (1994).
[42] F. Wooten, *Optical Properties of Solids* (Academic Press, New York, 1972).
[43] R. Lai, U. Happek, and A. J. Sievers, Phys. Rev. E **50**, R4294 (1994).
[44] R. Lai and A. J. Sievers, Nucl. Instrum. Methods Phys. Res., Sect. A **397**, 221 (1997).
[45] O. Grimm and P. Schmüser, TESLA FEL Report No. 2006-03.
[46] D. Mihalcea, C. L. Bohn, U. Happek, and P. Piot, Phys. Rev. ST Accel. Beams **9**, 082801 (2006).
[47] A. S. Kesar (private communication).
[48] S. Molloy, P. Emma, J. Frisch, R. Iverson, M. Ross, D. McCormick, M. Woods, S. Walston, and V. Blackmore, Report No. SLAC-PUB-12598, 2007.